Journal of Power Sources 243 (2013) 935–945

Contents lists available at SciVerse ScienceDirect

Journal of Power Sources

journal homepage: www.elsevier.com/locate/jpowsour

Investigation of the effects of methanol presence on characteristics of sulfonated aromatic electrolyte membranes: Molecular dynamics simulations

Ghasem Bahlakeh [a,*], Manouchehr Nikazar [a], Mohammad-Javad Hafezi [c], Mohammad Mahdi Hasani-Sadrabadi [b,c,*]

[a] Department of Chemical Engineering, Amirkabir University of Technology, Tehran, Iran
[b] Laboratoire de Microsystemes (LMIS4), École Polytechnique Fédérale de Lausanne (EPFL), CH-1015 Lausanne, Switzerland
[c] Department of Polymer Engineering and Color Technology, Amirkabir University of Technology, Tehran, Iran

HIGHLIGHTS

- SPPO membranes of different methanol concentrations were studied by MD simulation.
- SPPO membranes show phase separation on the uptake of methanol.
- Sulfonic acid groups were solvated more with water compared to methanol solvent.
- Larger solvent clusters formed at lower methanol concentrations.
- Methanol diffusion coefficient increased with increasing methanol concentration.

ARTICLE INFO

Article history:
Received 20 August 2012
Received in revised form
11 March 2013
Accepted 12 June 2013
Available online 21 June 2013

Keywords:
Polymer electrolyte membrane
Sulfonated poly(2,6-dimethyl-1,4-phenylene oxide) (SPPO)
Methanol
Molecular dynamics simulation

ABSTRACT

Effects of methanol solvent on characteristics of water–methanol solvated sulfonated poly(2,6-dimethyl-1,4-phenylene oxide) (SPPO) membranes were investigated at different methanol concentrations and temperatures using molecular dynamics simulations. Simulation results showed phase segregation of membrane on the uptake of methanol. Analysis of S–S RDFs revealed that the distance between sulfonic acid groups increased by increasing methanol concentration. Using RDFs of SPPO chains to solvent molecules, it was found that sulfonic acid groups were more solvated with water while aromatic backbone of SPPO exhibited stronger affinity toward methanol. From cluster size distribution examination, it was understood that larger solvent clusters formed at lower methanol concentrations. Diffusivity of water molecules decreased and that of methanol enhanced with an increase in methanol uptake. Calculated methanol diffusion coefficients were smaller in SPPO compared with Nafion, in agreement with experimental observations. Furthermore, increasing the temperature improved diffusivities for all permeants.

1. Introduction

Direct methanol fuel cells (DMFCs) have received considerable research attentions during past years as promising fuel cells for portable and stationary usages [1,2]. A key component of these fuel cells is a proton-conducting polymer electrolyte membrane (PEM) which separates anode and cathode parts. In this context, perfluorosulfonic acid polymeric membranes such as Nafion are the most widely applied DMFC membranes owing to possessing desirable features such as high chemical and mechanical stability with excellent ionic conductivity [3,4]. However, besides their high price and poor conductivity at elevated temperatures, high permeation of methanol feed through these ionomer membranes is a serious problem that drastically reduced the membrane selectivity (that is, the ratio of proton conductivity to methanol permeability) and limited their widespread applications. To overcome these problems, many attempts have been done for development of alternative polymeric membranes which can generate higher fuel cell performance compared to perfluorinated ionomers.

* Corresponding authors. Institute of Bioengineering, Swiss Federal Institutes of Technology, Lausanne (EPFL), 1015 Lausanne, Switzerland. Tel.: +41 76 745 8449.
E-mail addresses: ghasem.bahlakeh@gmail.com (G. Bahlakeh), mahdi.hasani@gmail.com, mahdi.hasani@gatech.edu (M.M. Hasani-Sadrabadi).

0378-7753/$ – see front matter © 2013 Elsevier B.V. All rights reserved.
http://dx.doi.org/10.1016/j.jpowsour.2013.06.066

Such candidate materials are mostly hydrocarbon polymers including poly(benzimidazole) (PBI), sulfonated poly(styrene) (SPS), sulfonated poly(ether ether ketone) (SPEEK), sulfonated poly(ether sulfone) (SPES), sulfonated poly(2,6-dimethyl-1,4-phenylene oxide) (SPPO) and so forth [5–8].

Thanks to their simple structure, favorable for polymer modifications, and satisfactory chemical, thermal and mechanical strength, SPPO PEMs have been widely investigated as promising DMFC membranes in various pure, composite and blend forms [7]. Tongwen et al. [9] reported the highest conductivity value of 0.015 S cm^{-1} for SPPO membranes with 28.7% sulfonation level using percolation theory and three-phase model (TPM). From atomic force microscopy analysis of SPPO membranes of different sulfonation levels, Guan et al. [10] observed continuous ionic regions in phase-segregated morphology of membrane, caused by higher water uptake of membrane at increased sulfonation degrees. Yang et al. [11] measured a comparable proton conductivity of 1.16×10^{-2} S cm^{-1} for SPPO membranes with that of Nafion 112 membrane at ambient temperature. In another study, Lu et al. [12] reported that hydrated composite membranes made of SPPO polymers and phosphosilicate gels yielded lower methanol crossover compared with Nafion 112 ionomer. Jung et al. [13] found the same behavior for conductivity and methanol permeability against sulfonation degree in SPPO membranes, suggesting that proton transport and methanol permeation mainly occur through the same domain inside the membrane. Lee et al. [14] measured lower methanol crossover in sulfonated crosslinked PPO (SCPPO) membranes with 30.1% degree of sulfonation as compared to Nafion 115 systems, which was ascribed to poor affinity of SPPO toward methanol and the lower size of clusters through which methanol transport takes place. Hasani-Sadrabadi et al. [15] obtained reduced methanol permeability in both pure and nanocomposite SPPO polymeric membranes with 2 wt% organically modified montmorillonite (MMT) clay in comparison with Nafion 117 membranes. More recent studies have demonstrated that the acid–base blends of SPPO membranes such as SPPO/PBI and SPPO/brominated poly(2,6-dimethyl-1,4-phenylene oxide) (BPPO) can also be used as potential PEMs for DMFCs, thanks to their reduced methanol permeability and enhanced membrane selectivity [16,17].

These experimental studies efficiently characterized two important transport properties of proton conductivity and methanol permeability in different SPPO membranes, which greatly affect performance of DMFCs in terms of membrane selectivity. In contrast to several experimental reports, simulation studies of these polymeric membranes were not carried out in earlier works. Simulation techniques, particularly atomistic molecular dynamics (MD) simulations, are very useful tools that help us attain detailed molecular level information concerning membrane characteristics, which cannot be easily achieved using experimental investigations, and discuss the observations from experiment in more details [18,19]. These simulation methods have been previously employed to explore the behavior of PEMs like Nafion and SPEEK under methanol aqueous solution conditions [20–24].

In the current research, it is intended to investigate the effects of methanol solvent molecules on several properties of pure SPPO membranes swollen by water–methanol mixture using MD simulations. To this purpose, a series of methanol concentrations were chosen for simulations, because experimental characterizations have shown that the concentration of methanol feed affects the selectivity of solvated PEM. Moreover, due to the dependence of membrane transport dynamics on operating temperature of DMFCs, MD simulations were also performed at different temperatures to examine the thermal effects on dynamics of solvated PEM. This study is an extension to our previous work which probed the behavior of SPPO membranes under varied water content conditions by means of MD simulations [25]. In contrast to several experimental and theoretical researches concerned with water–methanol solvated Nafion membranes [20–23,26–29], investigations of SPPO membranes swollen with methanol solutions were not addressed yet. Therefore, this simulation study will be focused on understanding of the methanol-related characteristics of SPPO membranes.

2. Simulation details

2.1. Atomistic models and amorphous-cell construction

Water–methanol solvated SPPO membranes containing different methanol concentrations were studied by means of classical MD simulation approaches to explore the effect of methanol solvent on several features of SPPO membranes. Five methanol weight percents (wt%) of 0, 20, 40, 60 and 80 were selected for MD simulations, where the methanol weight percent was defined as the ratio of weight of methanol solvent molecules to the sum of weight of methanol and water solvents. Also, four temperatures of 300, 318, 338 and 353 K were chosen to analyze the temperature effects on transport properties of permeants inside the membrane. MD simulations were conducted on five three-dimensional (3-D) cubic amorphous cells representing the behavior of solvated SPPO membranes under DMFC conditions. These amorphous cells consist of SPPO polymeric chains, water and methanol solvents, and hydronium ions (H_3O^+). 20 SPPO chains each with degree of polymerization of 20 (i.e., total number of non-sulfonated and sulfonated PPO monomers shown in Fig. 1) were applied for all simulation cells. Degree of sulfonation of 25% was used for SPPO chains, which was specifically considered here to be very close to the optimum degree of sulfonation of 27% determined by Hasani-Sadrabadi et al. [15], as used in our previous simulation study [25]. According to this sulfonation level, each SPPO polymeric chain contains 15 non-sulfonated and 5 sulfonated PPO monomers, which had random arrangement within the chain. With the assumption of complete ionization of sulfonic acid functional groups, the number of hydronium ions was set to be the same as the number of sulfonic acid groups to maintain the charge neutrality of the simulation cells. These hydronium ions were formed from combination of dissociated protons with water molecules, as used in earlier simulation studies of hydrated PEMs [18,19,21–25]. Total number of solvent molecules ($CH_3OH + H_2O$), which was maintained constant during simulations, corresponds to the number of water molecules in our previous MD simulation of hydrated SPPO membranes with water content of $\lambda = 9$ (λ is the ratio of number of water molecules to the fixed number of sulfonic acid groups) [25]. Detailed composition of amorphous cells for SPPO membranes with considered methanol concentrations was summarized in Table 1.

Initial 3-D amorphous simulation cells for SPPO membranes were constructed at a very low density of 0.005 g cm^{-3} by means of Amorphous-cell Builder module of Materials Studio software [30].

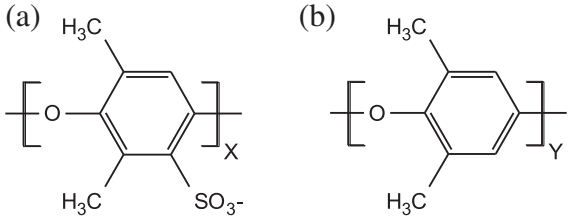

Fig. 1. Chemical structure of (a) fully ionized sulfonated PPO monomer and (b) non-sulfonated PPO monomer used for MD simulations. Degree of sulfonation (DS) is defined as: $DS\% = X/X + Y \times 100$.

Table 1
Composition of SPPO membranes used for MD simulations and equilibrated densities and cell sizes for methanol concentrations of 0, 20, 40, 60 and 80 wt%.

	Methanol concentration (wt%)				
	0	20	40	60	80
No. of SPPO chains	20	20	20	20	20
No. of H_3O^+	100	100	100	100	100
No. of H_2O	900	789	655	488	277
No. of CH_3OH	0	111	245	412	623
Total no. of atoms	10,240	10,240	10,240	10,240	10,240
Density (g cm^{-3})	1.0876	1.0890	1.0845	1.0784	1.0620
Cell size (Å)	48.3527	48.6686	49.1366	49.7194	50.5847

Such an initial density was particularly employed during cell construction process to prevent ring catenation problems due to the aromatic backbone of SPPO materials and accelerate the equilibration of simulation cells.

2.2. Force field parameters

All interaction parameters for SPPO chains were taken from DREIDING force filed reported by Mayo et al. [31], which is a generic force field on the basis of simple hybridization rules. This force field has been used successfully in the earlier MD simulations of proton exchange polymeric membranes [19,24,32–37]. Charge equilibration (QEq) algorithm described by Rappe and Goddard [38] was applied to assign partial atomic charges for all atoms in SPPO chains. Flexible 3-centered (F3C) force field from Levitt et al. [39] was utilized to model water molecules. Force field parameters for hydronium ions were taken from reports by Jang et al. [32]. Three-site potential model developed by Honma et al. [40] and OPLS-AA force field [41] were adopted to describe the methanol solvent interactions. For MD simulations, total potential energy of amorphous simulation cells was defined as follows:

$$E_{tot} = E_{bond} + E_{angle} + E_{dihedral} + E_{improper} + E_{vdW} + E_Q \quad (1)$$

where E_{tot}, E_{bond}, E_{angle}, $E_{dihedral}$, $E_{improper}$, E_{vdW} and E_Q are the total potential energy and its bond, angle, dihedral, improper, van der Waals (vdW) and electrostatic parts, respectively. Bonded interactions were described by their corresponding harmonic forms, and Lennard–Jones (LJ) 12–6 and coulomb potentials were used to represent the non-bonded vdW and electrostatic interactions. Therefore, equation (1) was expressed with the following functional form:

$$E_{tot} = \frac{1}{2}k_r(r-r_0)^2 + \frac{1}{2}k_\theta(\theta-\theta_0)^2 + \frac{1}{2}v_n(1-\cos[n(\varphi-\varphi_0)]) + \frac{1}{2}k_\psi(\psi-\psi_0)^2 + \sum_{i<j} 4\varepsilon_{ij}\left[\left(\frac{\sigma_{ij}}{r_{ij}}\right)^{12} - \left(\frac{\sigma_{ij}}{r_{ij}}\right)^{6}\right] + \sum_{i<j}\frac{q_i q_j}{r_{ij}} \quad (2)$$

where k_r, k_θ, v_n and k_ψ are bond, angle, dihedral and improper force constants, respectively. r_0, θ_0, ϕ_0 and ψ_0 represent the equilibrium values for bond, angle, dihedral and improper, respectively. n is periodicity, ε_{ij} and σ_{ij} are the vdW energy and size parameters for i and j atomic pair, r_{ij} is the distance between i and j atoms, and q_i and q_j are the partial atomic charges on i and j atoms. The vdW parameters for interactions between unlike pairs of atoms were obtained using geometric mean combination rule defined as equations (3) and (4):

$$\varepsilon_{ij} = \left(\varepsilon_{ii}\varepsilon_{jj}\right)^{1/2} \quad (3)$$

$$\sigma_{ij} = \left(\sigma_{ii}\sigma_{jj}\right)^{1/2} \quad (4)$$

2.3. MD simulation

During MD simulations, one of the crucial steps is the well equilibration of amorphous simulation cells, especially concerning complex aromatic systems which necessitate special considerations. In this regard, equilibration methods such as annealing and shrinking box have been used for simulations of polymeric membranes like poly(ethylene) and poly(dimethylsiloxane), and hydrated PEMs such as Nafion, SPEEK, SPPO and blend SPEEK–SPES [19,24,25,42–44]. In this study, since initial amorphous cells were created at a very low density, the shrinking box procedure was applied for equilibration phase of MD simulations.

All 3-D amorphous cells of water–methanol solvated SPPO membranes were first minimized using Conjugate Gradient method to remove the close contacts between atoms and make initial relaxation. MD simulations were then carried out under NPT ensemble for 10 ps, where the pressure was increased from 1 to 100 atm. This was followed by another NPT MD simulation performed over 1 ns during which the pressure was further increased from 100 to 150 atm. In these simulations, only bonded and repulsive part of non-bonded LJ interactions were included in total potential energy of the simulation systems expressed by equation (2). Then, NPT MD simulations were conducted at 150 atm for 10 ps where attractive part of non-bonded LJ interactions was also included. Simulations were continued for 50 ps at the same pressure of 150 atm with contribution of both non-bonded LJ and electrostatic interactions. Next, MD simulations were done in NPT ensemble at operating pressure of 1 atm for 10 ns. All these dynamics simulations were performed at 318 K. These successive NPT simulations were performed with the objective of accelerating the attainment of well equilibrated structures. Finally, the final structure obtained from equilibration phase was used as initial structure for production phase simulations which were conducted using NVT ensemble at 318 K for 2 ns. Molecular trajectories were used every 2000 steps during production simulations for subsequent analyses of membrane characteristics.

It should be noted that for amorphous cell with 40 wt% methanol concentration, which was selected to examine the temperature effects, all above MD simulations were first performed at the highest temperature of 353 K. For the lower temperatures, the final structure obtained at the end of production phase of a higher temperature was used as initial structure for its lower temperature, which was subjected to a 1.5 ns NPT simulation followed by a 100 ps NVT run before being used for production simulations.

Both equilibration and production phase of MD simulations were performed by using LAMMPS (large-scale atomic/molecular massively parallel simulator) open-source MD simulation code [45]. Periodic boundary conditions were imposed to all dimensions of the cubic simulation cells. Non-bonded interactions were

calculated with the use of 12 Å cutoff distance and long-range coulombic interactions were calculated by means of Particle–Particle Particle-Mesh (PPPM) method [46]. Newton's equation of motion was integrated by using velocity Verlet algorithm with a time step of 0.5 fs [47]. Temperature and pressure in all MD simulations were controlled using the Nose–Hoover method as thermostat and barostat with coupling parameters of 0.1 and 1 ps, respectively [48–50].

3. Results and discussion

3.1. Amorphous-cell equilibrium

Before analyzing the results obtained from production phase simulations, equilibration of the SPPO membranes solvated with water–methanol mixture was examined. In this regard, some widely used thermodynamic properties were checked as equilibrium criteria during MD simulations. These properties include density, temperature and potential energy of the 3-D amorphous cells, as they were applied by Chen et al. [22] in the study of Nafion membrane solvated by methanol aqueous solution. However, it should be noted that there has been no guarantee for fully equilibration of the resulting structures from MD simulations.

The predicted density and length of simulation cells for solvated SPPO membrane were provided in Table 1. It is seen that with increasing methanol concentration, the length of 3-D cells increases. As listed in Table 1, by an increase in weight percent of methanol, some of the water molecules inside the amorphous cell are replaced with methanol molecules and the number of methanol solvents is increased. Consequently, the increased length of 3-D cells of SPPO membrane is explained by the fact that although the total number of solvent molecules is the same for all methanol concentrations chosen here for SPPO membrane, the larger size of methanol compared to water causes the simulation cells for solvated membrane to enlarge more on the uptake of methanol solvents. By considering the solvation of SPPO membranes and comparing the simulated densities with the experimental values of 1.19 and 1.293 g cm^{-3} measured by Kruczek and Matsuura [51] and Hamad et al. [52] for dry SPPO membranes with 25.2% and 24.1% degree of sulfonation, respectively, it can be concluded that the estimated densities from MD simulations are reasonable for SPPO membrane solvated by methanol solution. Consequently, it is used as first indication of equilibrium. Moreover, Fig. 2 shows that the total potential energy and temperature of all simulation cells stay unchanged and their fluctuations are slight throughout the 2 ns dynamics simulation time, which can also act as another indication for reaching equilibrium condition.

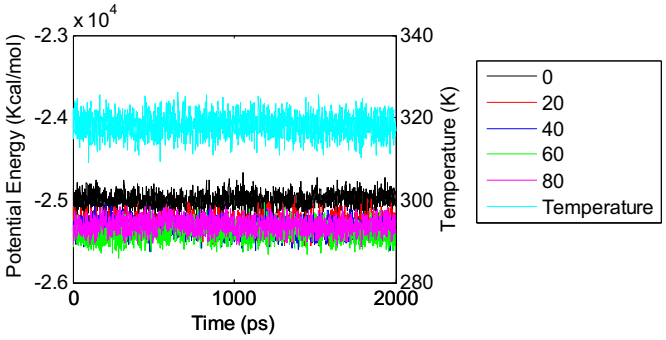

Fig. 2. Variation of total potential energy and temperature of the amorphous simulation systems with different methanol concentrations during 2 ns production phase MD simulations.

The final snapshots of the water–methanol solvated SPPO membranes obtained at the end of production stage were displayed in Fig. 3 for methanol concentrations of 20, 40, 60 and 80 wt%, which were visualized by means of Visual Molecular Dynamics (VMD) software [53].

In acid-type PEMs like SPPO, dynamical properties of membrane determine its potential for fuel cell applications. From experimental studies, it is well understood that these transport features strongly depend on membrane structural (static) characteristics such as degree of phase separation and clustering of solvent molecules under fuel cell conditions. Therefore, it is necessary to determine how the presence of methanol solvent molecules affects the structure of solvated SPPO membrane. For this purpose, different analyses, such as correlation for solvent molecules and SPPO chains and solvent cluster size distribution, were done in next section to achieve deeper insights into the morphologies illustrated in Fig. 3.

3.2. Static property analysis

To investigate the local structure of the water–methanol solvated SPPO membranes under different methanol concentration conditions, the radial distribution function (RDF, also called pair correlation function) was employed. For a certain pair of *A* and *B* atoms, indicates the probability distribution of *B* atoms around central *A* atoms and is defined according to equation (5):

$$g_{A-B}(r) = \frac{\left(\frac{n_B}{4\pi r^2 \Delta r}\right)}{\left(\frac{N_B}{V}\right)} \quad (5)$$

where n_B is the number of atoms located around *A* atoms inside a spherical shell of thickness Δr, N_B is the total number of *B* atoms applied for amorphous cell and *V* is the equilibrated volume of amorphous cell, as its length was provided in Table 1 for all methanol concentrations.

Fig. 4 shows the RDFs of sulfur–sulfur (S–S) atomic pair in sulfonic acid groups for varied methanol concentrations in solvated SPPO membranes. It is observed that with the increase in methanol concentration, the first pronounced peak is occurred at farther distances, which means that the separation distance between sulfonic acid groups attached to SPPO chains is increased. This behavior is attributed to the replacement of the water molecules in solvation shell of sulfonic acid groups with higher number of methanol molecules at increased weight percent of methanol which pushes away anionic sulfonic acid groups from each other. The non-monotonic behavior in peak position against methanol content of membrane is likely because of decreasing number of water molecules, and the presence of mixed water–methanol solvents which can lead to inhomogeneous methanol distribution inside the solvated membrane.

Methanol solvation of sulfonic acid groups is explained by means of the correlation of sulfur and oxygen atoms in sulfonic acid group with respect to both oxygen atom (Om) and methyl group (Cm) in methanol. Fig. 5(a) and (b) displays the RDFs of sulfur atoms of sulfonic acid groups toward the oxygen atoms and methyl groups of methanol solvent, respectively, for methanol concentrations from 20 to 80 wt%. A peak in S–Om RDFs occurs at 3.66 Å, while it is observed in the range of 4.26–4.86 Å for S–Cm RDFs. It is seen that with increasing the methanol concentration, the height of the observed peak enhances for both S–Om and S–Cm RDFs. Since an increase in methanol concentration is accompanied by a decrease in the number of water molecules, the higher peak intensity at higher methanol uptakes of membrane is owing to the lower water screening effect on methanol molecules. Parts (c) and (d) in Fig. 5

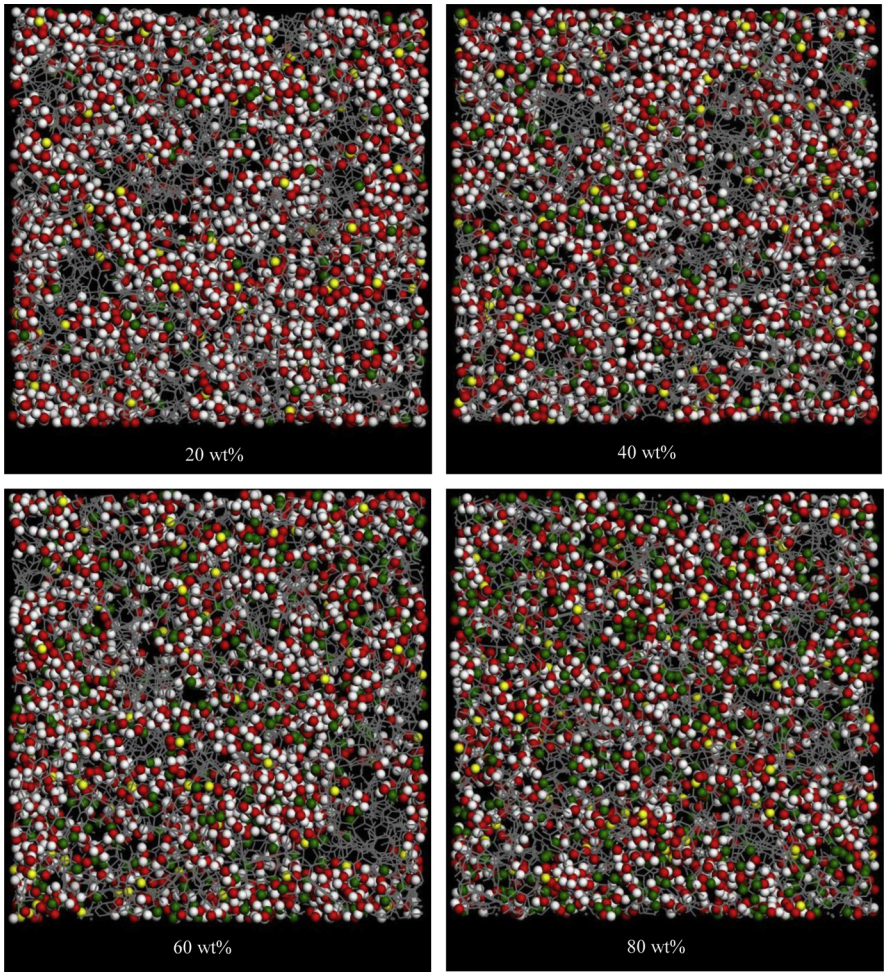

Fig. 3. Final snapshots of water–methanol solvated SPPO membranes for 20, 40, 60 and 80 wt% methanol concentrations obtained at the end of production phase MD simulations. For all membranes the color code is: polymeric chains backbone: gray; water oxygen, hydronium ion oxygen, sulfonic acid oxygen and methanol oxygen atoms: red; sulfur atoms: yellow; water hydrogen, hydronium ion hydrogen and methanol hydroxyl hydrogen atoms: white and methanol methyl groups (CH_3): green. (For interpretation of the references to color in this figure legend, the reader is referred to the web version of this article.)

indicate the Os–Om and Os–Cm RDFs, respectively. A peak with greater height is observed at 2.82 and 3.42 Å in Os–Om and Os–Cm RDFs, respectively, for all values of methanol concentration. The trend of these two RDFs against methanol concentration is the same as that of S–Om and S–Cm RDFs. Existence of a high peak in RDFs of sulfonic acid group with regards to methanol, which is as a result of the hydrogen bonding interaction between hydroxyl hydrogen atom of methanol and sulfonic acid oxygen atoms, implies the appearance of methanol solvation shell around anionic sulfonic acid groups. Therefore, it could be inferred that the presence of methanol molecules can help the phase segregation of SPPO membranes. To attain quantitative insight into the presence of methanol molecules in the vicinity of sulfonic acid groups, their coordination number was calculated by integrating the S–Om and Os–Om RDFs using the following equation:

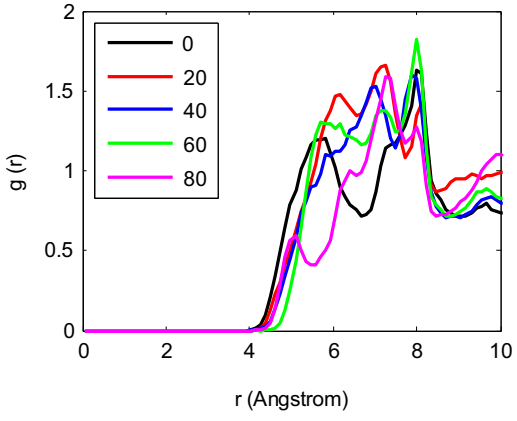

Fig. 4. RDFs of sulfur–sulfur atomic pair of sulfonic acid group for different methanol concentrations at 318 K.

$$n_B = 4\pi \frac{N_B}{V} \int r^2 g_{A-B}(r)\, \mathrm{d}r \tag{6}$$

where n_B is the coordination number of B atoms around central A atoms. Table 2 lists the calculated coordination number for methanol oxygen atoms around sulfur and oxygen atoms in sulfonic acid group. It is found that sulfonic acid groups become more methanol solvated by changing the methanol concentration from 20 to 80 wt%.

Fig. 6(a) and (b) presents the RDFs for sulfonic acid sulfur atoms to the oxygen atoms in water (Ow) and hydronium ion (Oh). In the case of S–Ow RDFs, an intensified peak is observed at 3.66 Å for 0 and 20 wt% and 3.54 Å for 40, 60 and 80 wt% methanol concentration. For S–Oh RDFs, the peak with significant height occurs at

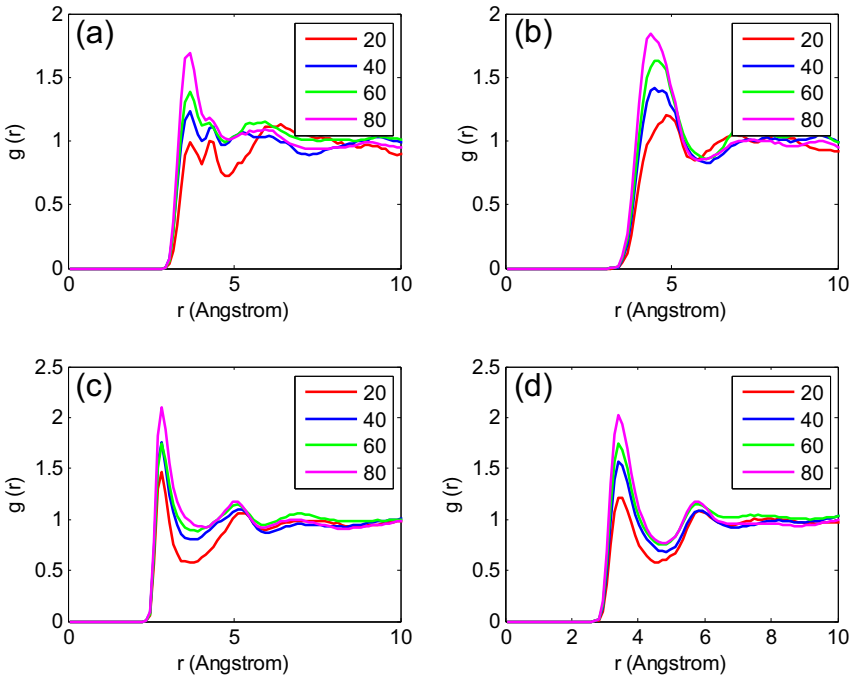

Fig. 5. RDFs of (a) sulfur(sulfonic acid group)–oxygen(methanol), (b) sulfur(sulfonic acid group)–methyl(methanol), (c) oxygen(sulfonic acid group)–oxygen(methanol) and (d) oxygen(sulfonic acid group)–methyl(methanol) for different methanol concentrations at 318 K.

approximately 3.3 Å for 0 and 60 wt% and 3.42 Å for 20, 40 and 80 wt% methanol uptake. The peak height in both RDFs increases as the concentration of methanol solvent is increased, which is ascribed to weaker water solvent effect on both water and hydronium ion at increased methanol uptake values. From comparison of the intensity of heightened peak in S–Om (Fig. 5(a)) and S–Ow RDFs, it can be seen that the peak intensity is greater in S–Ow RDFs than in S–Om RDFs. Hence, it could be deduced that in SPPO membranes swollen with water–methanol mixture, where solvents compete to surround sulfonic acid groups, water molecules are more able to solvate the sulfonic acid groups as compared to methanol and thereby greater number of water molecules can be found in the solvent shell formed around sulfonic acid groups, as shown in Table 2. According to results presented in Table 2, coordination number for hydronium ions around sulfonic acid group first increases and then slightly declines with enhancing methanol weight percent. The initial increase is rationalized by the weakening trend of water solvent effect on hydronium ions which holds hydronium ions closer to sulfonic acid groups, and the decrease is caused by the pronounced methanol solvation around sulfonic acid groups at higher methanol concentrations which moves hydronium ions away from sulfonic acid groups by decreasing their electrostatic interactions.

In summary, from the observed peak in RDFs for sulfonic acid group with respect to methanol, water and hydronium ion, it is inferred that SPPO membranes solvated with aqueous solution of methanol demonstrate phase separated microstructure consisting of hydrophilic (ionic) and hydrophobic regions, the same as that observed in our recent MD simulation studies of water solvated pure SPEEK and SPPO as well as blend SPEEK-SPES membranes [18,19,25]. This observation is consistent with the experimental results about alcohol solvated perfluorinated membranes reported by Saito et al. [26].

Table 2
Coordination number of solvent molecules and hydronium ion around sulfonic acid groups for different methanol concentrations at 318 K.

Atomic pair	Distance (Å)	Methanol concentration (wt%)				
		0	20	40	60	80
S–Om	0–5		0.31	0.85	1.5	2.3
Os–Om	0–3.9		0.14	0.41	0.7	1.15
S–Ow	0–5	4.74	4.3	3.5	2.7	1.42
S–Oh	0–4	0.63	0.64	0.68	0.81	0.8

To examine the interaction of solvent molecules with backbone of SPPO polymers, correlation of aromatic carbon (C) atoms in rigid backbone of SPPO with oxygen atom of solvents was analyzed for all levels of methanol concentration. Fig. 7(a) and (b) exhibits the changes in C–Ow and C–Om RDFs, respectively, against methanol uptake of solvated membrane. As displayed, the RDFs of C–Ow increase with the distance but their height remains lower than unity which is due to the hydrophobic nature of aromatic carbon atoms in SPPO backbone. On the contrary, the C–Om RDFs demonstrate a peak at approximately 5–6 Å, an observation resulting from the LJ interactions of methyl group in methanol solvent with aromatic carbon in backbone of SPPO chains. Therefore, it is inferred that unlike the water solvents which only solvate the sulfonic acid groups, methanol solvent molecules are able to surround both hydrophilic sulfonic acid groups and hydrophobic aromatic backbones in SPPO chains. With varying methanol concentration from 20 to 80 wt%, the magnitude of C–Om RDFs is observed to decrease which could be attributed to the increased migration of methanol solvents within the membrane at higher values of methanol concentration, as discussed in next section.

Solvation of hydronium ions by water and methanol was described in terms of RDFs of hydronium ion oxygen atoms (Oh) with regards to water and methanol oxygen atoms for different levels of methanol uptake, as demonstrated in Fig. 8(a) and (b). The trend for height of peak occurred at 2.58 Å against methanol uptake is the same for both RDFs, that is, stronger peak at higher methanol solvent concentrations thanks to reduced water solvent effect. The intensity of observed peak is more pronounced in Oh–Ow RDFs in

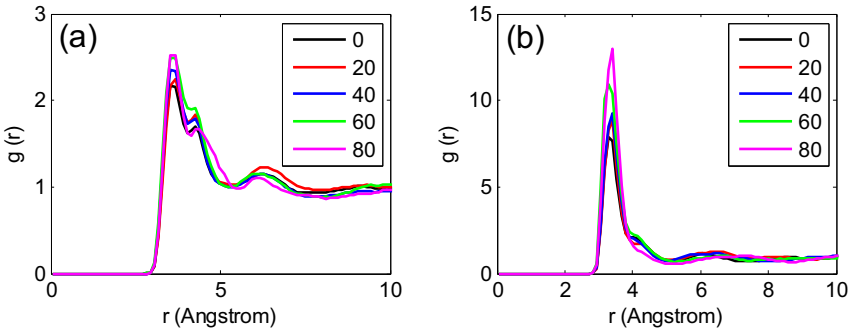

Fig. 6. RDFs of (a) sulfur(sulfonic acid group)–oxygen(water) and (b) sulfur(sulfonic acid group)–oxygen(hydronium ion) for different methanol concentrations at 318 K.

comparison with Oh–Om RDFs, which reflects the fact that in SPPO membranes solvated by water and methanol, hydronium ions are surrounded more with water molecules. Quantitative comparison of solvation capacity of solvents was done by computing the water and methanol coordination number within first solvent shell around hydronium ions (i.e. 3 and 4 Å for Oh–Ow and Oh–Om RDFs, respectively). The coordination numbers were calculated as 2.34, 2.06, 1.64 and 1.12 for water, and 0.17, 0.26, 0.17 and 0.28 for methanol at 20, 40, 60 and 80 wt% methanol concentrations, respectively. These results further describe the stronger solvation ability of water compared to methanol.

Fig. 9(a) exhibits the methanol concentration dependence of RDFs of water oxygen to water oxygen (Ow–Ow). For all concentrations of methanol, a strong peak is observed at a distance of 2.82 Å whose height is increased by an enhancement in methanol weight percent. This behavior is caused by the weaker water screening effect on water molecules at higher methanol concentrations. Enhanced peak in Ow–Ow RDFs reveals the fact that water molecules tend to form aqueous clusters inside the membrane even in the presence of methanol molecules. RDFs for oxygen atoms in methanol solvent toward methanol oxygen (Om–Om) and water oxygen atoms (Om–Ow) were illustrated in parts (b) and (c) of Fig. 9. In these RDFs, a pronounced peak is noted at 2.7 Å, where its behavior against methanol concentration is similar to that of Ow–Ow RDFs. Appearance of intensified peak in Om–Om and Om–Ow RDFs suggests the tendency of methanol solvent molecules to aggregate not only with each other but also with water molecules and form solvent clusters. These results are in accordance with observations from snapshots of solvated SPPO membranes provided in Fig. 3. To quantitatively evaluate the clustering tendency of solvents at various methanol concentrations, the coordination number of water molecules for water and methanol solvents, and methanol molecules for methanol solvent was computed by integration of corresponding RDFs up to first minimum (3.42 Å for all three RDFs) and plotted in Fig. 9(d). As indicated, with the increase in uptake of methanol, the number of water molecules surrounding both water and methanol solvents become diminished, an observation on account of smaller number of water solvent molecules at higher methanol concentration. However, methanol molecules are more solvated by methanol molecules at increased weight percents of methanol. Formation of solvent clusters within the SPPO membranes solvated with mixture of water and methanol further confirms the phase segregation of membrane.

Cluster size distribution of solvent molecules was studied to quantify the solvent clusters observed in Fig. 3. Also, to further analyze the distribution of water molecules inside the solvated membrane, their own clusters (i.e., water solvent without considering methanol) were investigated. In computation of size of solvent cluster, hydronium ions were not distinguished from solvent molecules. Two solvent molecules were assumed to be in the same cluster if the intermolecular distance between their oxygen atoms (i.e., oxygen atoms in hydronium ion, water or methanol) is less than the given cutoff radius. Since a pronounced peak in RDF implies the clustering tendency of molecules, a 3.5 Å cutoff distance, which is about location of first minimum in RDFs among water, methanol and hydronium ion, was utilized to consider solvent molecules and hydronium ions in cluster formation. The average number of molecules in a certain cluster was determined from the product of time-averaged number of that cluster (that is, the average occurrence number of a cluster during MD simulation) and its size. To better describe the methanol concentration impacts on solvent cluster size distribution, clusters containing less than 100 molecules were identified as small clusters, and those with more than 400 molecules were recognized as large clusters. Fig. 10(a) and (b) shows the time-averaged cluster size distribution for small and large water solvent clusters, respectively, inside the SPPO membranes for varied methanol concentrations. It is seen that with an increase in methanol concentration from 0 to 80 wt%, the average number of molecules in small clusters increases, while that in large clusters decreases, an

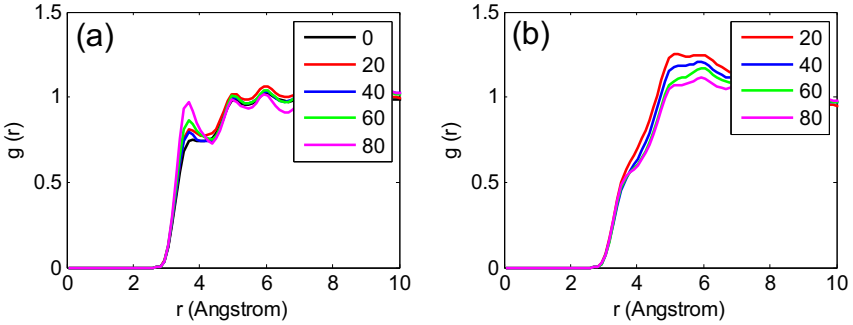

Fig. 7. RDFs of (a) aromatic carbon(backbone)–oxygen(water) and (b) aromatic carbon(backbone)–oxygen(methanol) for different methanol concentrations at 318 K.

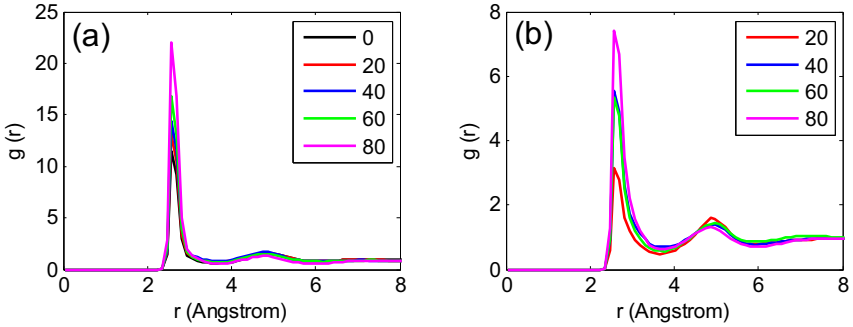

Fig. 8. RDFs of (a) oxygen(hydronium ion)–oxygen(water) and (b) oxygen(hydronium ion)–oxygen(methanol) for different methanol concentrations at 318 K.

expected result because of the reduced number of water solvent molecules at enhanced methanol uptake values. It is interesting that despite the constant number of solvent molecules for all methanol concentrations, similar behavior is observed for mixed water–methanol solvent cluster size distribution against methanol concentration, as displayed in parts (c) and (d) of Fig. 10. For the case of large clusters, as the methanol concentration is enhanced, the observed cluster size decreases and solvents are found in clusters of smaller size. In addition, distribution of solvent cluster size becomes broader in increasingly methanol solvated membranes. Such observations are assigned to replacement of water molecules with methanol solvents which have weaker hydrogen bonding interaction with constituents of hydrophilic phase (i.e., water, methanol, hydronium ions and sulfonic acid groups) in comparison with water. Furthermore, interaction of methanol molecules with hydrophobic backbone of SPPO is another reason for appearance of smaller solvent clusters at higher methanol concentrations.

Schlick and Alonso-Amigo [27] and Li and Schlick [28] reported smaller solvent clusters and less phase segregation in Nafion membranes solvated by methanol or water–methanol mixture with higher methanol concentration (>20% by volume) compared with those swollen by water–methanol mixture of less methanol content or pure water solvent. Consequently, obtained simulation results of smaller solvent clusters at higher methanol concentrations in water–methanol solvated SPPO membranes follow the experimental observations reported for Nafion membranes solvated by methanol aqueous solution.

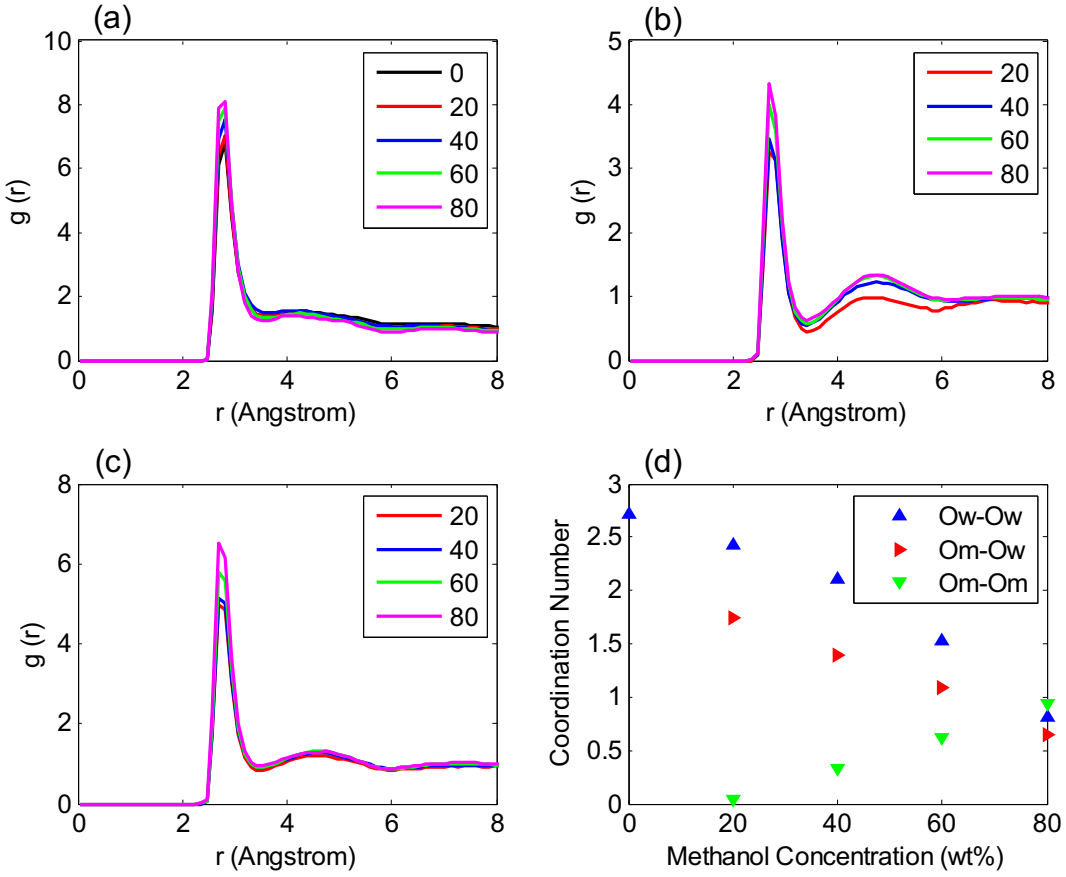

Fig. 9. RDFs of (a) oxygen(water)–oxygen(water), (b) oxygen(methanol)–oxygen(methanol) and (c) oxygen(methanol)–oxygen(water); (d) coordination number of water molecules around water and methanol, and methanol molecules around methanol for different methanol concentrations at 318 K.

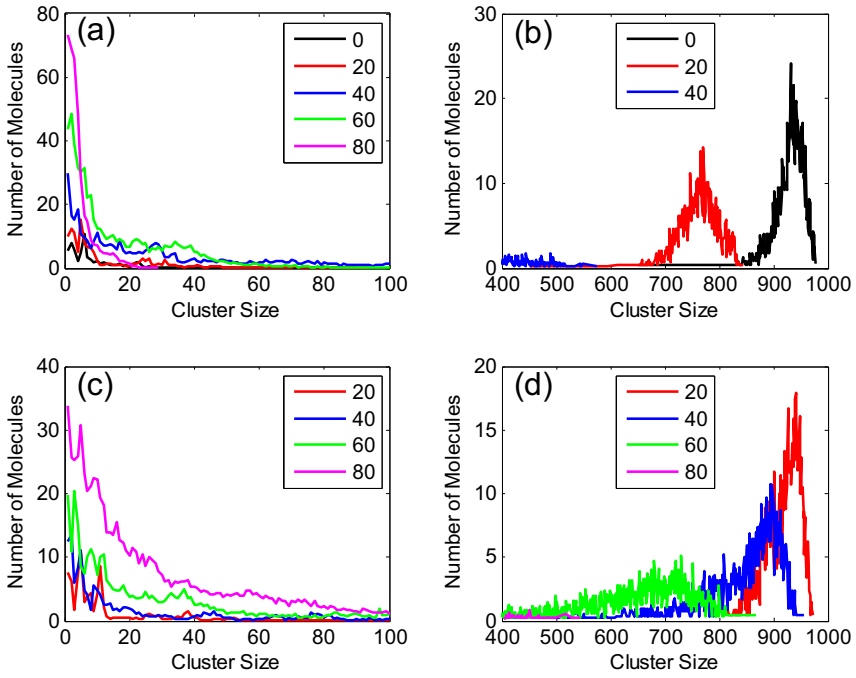

Fig. 10. Average cluster size distribution of (a) small and (b) large water solvent clusters, and (c) small and (d) large water/methanol solvent clusters inside the water–methanol solvated SPPO membranes for different methanol concentrations at 318 K.

3.3. Dynamic property analysis

Dynamical characteristics of SPPO membranes solvated by aqueous solution of methanol molecules were analyzed by the evaluation of diffusivity of permeants (i.e. hydronium ion, water and methanol) inside the membrane. Additionally, to examine the effect of temperature on membrane dynamics, diffusivities in SPPO membranes with 40 wt% methanol concentration were determined at temperatures considered here. In order to calculate the hydronium ion, water and methanol diffusion coefficients, first, their corresponding mean squared displacement (*MSD*) was estimated using the following equation:

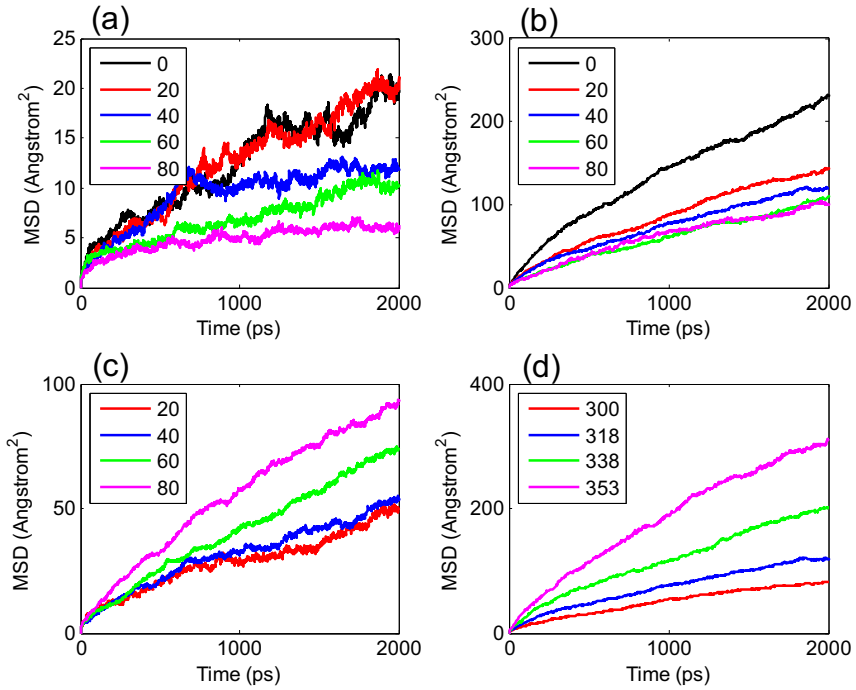

Fig. 11. *MSD* of (a) hydronium ions, (b) water molecules and (c) methanol molecules inside the water–methanol solvated SPPO membranes for different methanol concentrations at 318 K; (d) *MSD* of water molecules in SPPO membranes with 40 wt% methanol concentration at different temperatures.

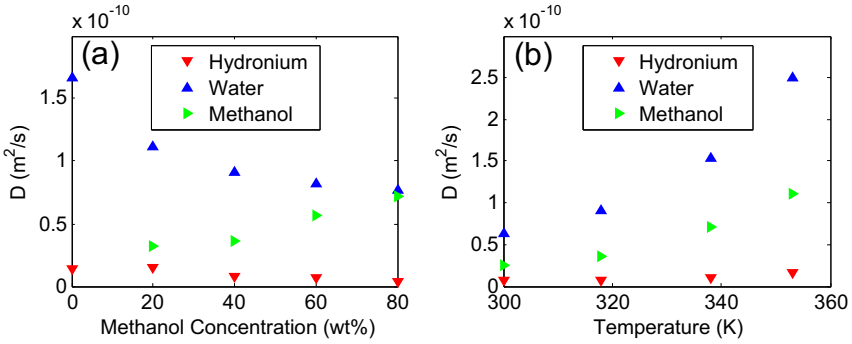

Fig. 12. Diffusion coefficients of hydronium ions, water molecules and methanol molecules (a) in SPPO membranes for different methanol concentrations at 318 K and (b) in SPPO membranes with 40 wt% methanol concentration at different temperatures.

$$MSD(t) = \left\langle \left(r_j(t) - r_j(0)\right)^2 \right\rangle = \frac{1}{N}\sum_{j=1}^{N}\left[\left(r_j(t) - r_j(0)\right)^2\right] \tag{7}$$

where N is the total number of particles j, and $r_j(t)$ and $r_j(0)$ are the positions of the particle j at time and beginning of production runs, respectively. Diffusion coefficients D were then computed from the slope of *MSD* curves or using Einstein relation defined by equation (8):

$$D = \frac{1}{6}\lim_{t\to\infty}\frac{\mathrm{d}MSD(t)}{\mathrm{d}t} = \frac{1}{6N}\lim_{t\to\infty}\frac{\mathrm{d}}{\mathrm{d}t}\sum_{j=1}^{N}\left[\left(r_j(t) - r_j(0)\right)^2\right] \tag{8}$$

Fig. 11(a)–(c) displays the *MSD* curves of hydronium ion, water and methanol, respectively, for various amounts of methanol concentration at 318 K. The *MSD* curves for all permeants demonstrate almost a linear behavior which reveals the continuous mobility of hydronium ion and water as well as methanol through the SPPO membrane. The *MSD* of water molecules in SPPO membranes of 40 wt% methanol concentration as a function of temperature was illustrated in part (d) of Fig. 11. The simulation results for the diffusion coefficients of hydronium ion, water and methanol for varied concentrations of methanol were provided in Fig. 12(a). As exhibited, with an increase in methanol concentration from 0 to 80 wt%, the diffusion coefficient for water molecules is observed to decrease. This trend in water diffusivity arises from the reduced number of water molecules and smaller size of clusters at higher values of methanol concentration. On the contrary, diffusion coefficient of the methanol solvents increases by an increase in methanol uptake of SPPO membrane which is because of the facts that the presence of greater number of methanol molecules and larger simulation cells at enhanced methanol concentrations accelerate the overall movement of methanol within the membrane. Diffusion coefficients of hydronium ions are lower than those of water and methanol molecules. One reason for this observation is that calculation of hydronium ion diffusivity via above equation only includes the vehicular mechanism of proton diffusion, while proton transport through solvated membrane occurs by vehicular and hopping mechanisms. Furthermore, the strong electrostatic interactions between sulfonic acid groups and hydronium ions further decrease the mobility of hydronium ions within the water–methanol solvated SPPO membrane. Since there have been no reported experimental diffusivities of these molecules through the water–methanol solvated SPPO membranes, it is not possible to make a comparison between simulation and experiment. The change in diffusion coefficient of hydronium ion against methanol concentration is slight in comparison with that of water and methanol. It should be noticed that the obtained diffusivity of hydronium ion represents the vehicular type proton condition since calculation of hydronium ion diffusion coefficient using equation (8) only includes the vehicular mechanism for proton transport. As the methanol concentration is enhanced, hydronium ion diffusivity first increases and then decreases slightly. Although the decreased number of water molecules may decrease the diffusivity of hydronium ion, the fact that the total number of solvent molecules is constant during simulations can prevent from the significant reduction in hydronium ion mobility.

Fig. 12(b) illustrates the diffusivities of hydronium ion, water and methanol in SPPO membranes solvated by 40 wt% methanol solution at temperatures of 300, 318, 338 and 353 K. It is found that increasing the temperature leads to increased diffusion coefficients for all permeants, as a result of enhanced mobility of permeants at higher temperature conditions.

The trend in diffusion coefficient of permeants as a function of methanol concentration and temperature found in this study for solvated SPPO membranes is similar to the simulation results reported by Chen et al. [22] for water–methanol solvated Nafion membranes. These authors predicted the methanol diffusion coefficients of 0.0829, 0.0898 and 0.0993 $\times$ 10^{-8} m^2 s^{-1}, respectively, for solvated Nafion membranes containing 11.23, 21.40 and 46.92 wt% methanol concentration at 323 K. Although these methanol concentrations are not the same as those studied in this work, however, by making a comparison between the reported methanol diffusion coefficients for Nafion and those obtained for SPPO membrane (i.e., 0.0032, 0.0033, 0.0057 and 0.0072 $\times$ 10^{-8} m^2 s^{-1} for 20, 40, 60 and 80 wt% methanol concentration at 318 K), it is found that the diffusion coefficients for methanol solvent in SPPO membrane are lower than the corresponding values in Nafion. Consequently, from this observation, it could be inferred that the SPPO membranes exhibit lower methanol transport property compared to conventional Nafion membrane, which accords well with the experimentally obtained lower methanol permeability in pure SPPO membranes compared to Nafion membrane [15].

4. Conclusion

Classical MD simulation techniques were applied to investigate the effects of methanol solvent on various properties of polymeric membranes based on SPPO materials, solvated with five different methanol concentrations of 0, 20, 40, 60 and 80 wt%. The transport of hydronium ion, water and methanol solvents within the membrane was also examined at different temperatures of 300, 318, 338 and 353 K. Simulation results exhibited the phase segregation behavior of SPPO membranes on the uptake of methanol solvent molecules.

To examine the distribution of hydronium ions, water and methanol solvents inside the membrane, and their correlations with respect to sulfonic acid groups and aromatic backbone of SPPO materials, RDF analysis was performed. From evaluation of S–S RDFs, it was found that with increasing methanol concentration, the average distance between neighboring hydrophilic sulfonic acid groups increased. By comparing the solvation ability of solvent molecules for sulfonic acid groups and backbone of SPPO, it was understood that the sulfonic acid groups were surrounded more by water molecules compared to methanol solvents, while the aromatic backbone of SPPO was found to be hydrophobic and showed greater affinity toward the methanol.

Hydronium ion RDFs with water and methanol solvents suggested the stronger solvation of hydronium ions with water molecules in comparison with methanol. Additionally, RDFs for water and methanol solvents demonstrated the clustering of solvents. Simulation results of solvent cluster size distribution showed that with an increase in concentration of methanol, size of clusters decreased.

Diffusion coefficients of water molecules within the SPPO membranes decreased by increasing methanol concentration, while those of methanol solvents enhanced. The variation in diffusion coefficients of hydronium ions against methanol concentration was slight. Furthermore, diffusivity for all permeants enhanced as the temperature increased. The calculated methanol diffusion coefficients in SPPO membranes were smaller than the reported values in Nafion membrane, which indicated the reduced transport of methanol in SPPO membranes compared to that of Nafion.

Solvated pure SPPO membranes because of their desirable features such as phase separated microstructure and formation of solvent clusters as well as lower methanol transport property could be taken into account as a candidate PEM for use in DMFCs.

Acknowledgment

This research was financially supported by Iran Renewable Energy Organization (SUNA). The authors gratefully acknowledge the use of High Performance Computing Research Center (HPCRC) of Amirkabir University of Technology.

References

[1] X. Ren, P. Zelenay, S. Thomas, J. Davey, S. Gottesfeld, J. Power Sources 86 (2000) 111–116.
[2] S.K. Kamarudin, F. Achmad, W.R.W. Daud, Int. J. Hydrogen Energy 34 (2009) 6902–6916.
[3] K.A. Mauritz, R.B. Moore, Chem. Rev. 104 (2004) 4535–4586.
[4] G. Alberti, M. Casciola, Solid State Ionics 145 (2001) 3–16.
[5] M. Rikukawa, K. Sanui, Prog. Polym. Sci. 25 (2000) 1463–1502.
[6] M. Gil, X. Ji, X. Li, H. Na, J.E. Hampsey, Y. Lu, J. Membr. Sci. 234 (2004) 75–81.
[7] T. Xu, D. Wu, L. Wu, Prog. Polym. Sci. 33 (2008) 894–915.
[8] H. Ahmad, S.K. Kamarudin, U.A. Hasran, W.R.W. Daud, Int. J. Hydrogen Energy 35 (2010) 2160–2175.
[9] X. Tongwen, Y. Weihua, H. Binglin, Chem. Eng. Sci. 56 (2001) 5343–5350.
[10] R. Guan, C. Gong, D. Lu, H. Zou, W. Lu, J. Appl. Polym. Sci. 98 (2005) 1244–1250.
[11] S. Yang, C. Gong, R. Guan, H. Zou, H. Dai, Polym. Adv. Technol. 17 (2006) 360–365.
[12] D. Lu, W. Lu, C. Li, J. Liu, R. Guan, Polym. Bull. 58 (2007) 673–682.
[13] B. Jung, B. Kim, J.M. Yang, J. Membr. Sci. 245 (2004) 61–69.
[14] J.S. Lee, C.H. Jung, S.Y. Jo, J.H. Choi, I.T. Hwang, Y.C. Nho, Y.M. Lee, J. Polym. Sci. A: Polym. Chem. 48 (2010) 2725–2731.
[15] M.M. Hasani-Sadrabadi, S.H. Emami, H. Moaddel, J. Power Sources 183 (2008) 551–556.
[16] A.H. Haghighi, M.M. Hasani-Sadrabadi, E. Dashtimoghadam, G. Bahlakeh, S.E. Shakeri, F.S. Majedi, S. Hojjati Emami, H. Moaddel, Int. J. Hydrogen Energy 36 (2011) 3688–3696.
[17] T. Xu, D. Wu, S.-J. Seo, J.-J. Woo, L. Wu, S.-H. Moon, J. Appl. Polym. Sci. 124 (2012) 3511–3519.
[18] G. Bahlakeh, M. Nikazar, M.-J. Hafezi, E. Dashtimoghadam, M.M. Hasani-Sadrabadi, Int. J. Hydrogen Energy 37 (2012) 10256–10264.
[19] G. Bahlakeh, M. Nikazar, M. Mahdi Hasani-Sadrabadi, J. Membr. Sci. 429 (2013) 384–395.
[20] A. Vishnyakov, A.V. Neimark, J. Phys. Chem. B 105 (2001) 7830–7834.
[21] S. Urata, J. Irisawa, A. Takada, W. Shinoda, S. Tsuzuki, M. Mikami, J. Phys. Chem. B 109 (2005) 17274–17280.
[22] P.Y. Chen, C.P. Chiu, C.W. Hong, J. Electrochem. Soc. 155 (2008) B1255–B1263.
[23] X. Ji, L. Yan, S. Zhu, L. Zhang, W. Lu, J. Phys. Chem. B 112 (2008) 15616–15627.
[24] C.V. Mahajan, V. Ganesan, J. Phys. Chem. B 114 (2010) 8357–8366.
[25] G. Bahlakeh, M. Nikazar, Int. J. Hydrogen Energy 37 (2012) 12714–12724.
[26] M. Saito, S. Tsuzuki, K. Hayamizu, T. Okada, J. Phys. Chem. B 110 (2006) 24410–24417.
[27] S. Schlick, M.G. Alonso-Amigo, Macromolecules 22 (1989) 2634–2641.
[28] H. Li, S. Schlick, Polymer 36 (1995) 1141–1146.
[29] C.E. Tsai, B.J. Hwang, Fuel Cells 7 (2007) 408–416.
[30] Accelrys Software Inc. SD, 2009.
[31] S.L. Mayo, B.D. Olafson, W.A. Goddard, J. Phys. Chem. 94 (1990) 8897–8909.
[32] S.S. Jang, V. Molinero, T. Cagin, W.A. Goddard, J. Phys. Chem. B 108 (2004) 3149–3157.
[33] P.Y. Chen, C.P. Chiu, C.W. Hong, J. Power Sources 194 (2009) 746–752.
[34] G. Brunello, S.G. Lee, S.S. Jang, Y. Qi, J. Renew. Sustain. Energy 1 (2009) 033101–033114.
[35] G.F. Brunello, W.R. Mateker, S.G. Lee, J.I. Choi, S.S. Jang, J. Renew. Sustain. Energy 3 (2011) 043111–043116.
[36] C.H. Cheng, P.Y. Chen, C.W. Hong, J. Electrochem. Soc. 155 (2008) B435–B442.
[37] R. Devanathan, A. Venkatnathan, M. Dupuis, J. Phys. Chem. B 111 (2007) 13006–13013.
[38] A.K. Rappe, W.A. Goddard, J. Phys. Chem. 95 (1991) 3358–3363.
[39] M. Levitt, M. Hirshberg, R. Sharon, K.E. Laidig, V. Daggett, J. Phys. Chem. B 101 (1997) 5051–5061.
[40] T. Honma, C.C. Liew, H. Inomata, K. Arai, J. Phys. Chem. A 107 (2003) 3960–3965.
[41] W.L. Jorgensen, D.S. Maxwell, J. Tirado-Rives, J. Am. Chem. Soc. 118 (1996) 11225–11236.
[42] R.M. Sok, H.J.C. Berendsen, W.F. Van Gunsteren, J. Chem. Phys. 96 (1992) 4699–4704.
[43] N.F.A.V. Vegt, W.J. Briels, M. Wessling, H. Strathmann, J. Chem. Phys. 105 (1996) 8849–8857.
[44] A. Vishnyakov, A.V. Neimark, J. Phys. Chem. B 105 (2001) 9586–9594.
[45] S.J. Plimpton, J. Comput. Phys. 117 (1995) 1–19.
[46] R.W. Hockney, J.W. Eastwood, Computer Simulation Using Particles, McGraw-Hill, New York, 1981.
[47] W.C. Swope, H.C. Andersen, P.H. Berens, K.R. Wilson, J. Chem. Phys. 76 (1982) 637–649.
[48] S. Nose, J. Chem. Phys. 81 (1984) 511–519.
[49] S. Nose, Mol. Phys. 52 (1984) 255–268.
[50] S. Nose, Mol. Phys. 57 (1986) 187–191.
[51] B. Kruczek, T. Matsuura, J. Membr. Sci. 167 (2000) 203–216.
[52] F.A. Hamad, G. Chowdhury, T. Matsuura, J. Membr. Sci. 191 (2001) 71–83.
[53] W. Humphrey, A. Dalke, K. Schulten, J. Mol. Graph. 14 (1996) 33–38.